

IFUP-TH 23/96
 LPTHE 95/24
 Liverpool U. LTH 398
 FERMILAB-PUB-97/169-T
 Edinburgh 97/5

α_s from the Non-perturbatively Renormalised Lattice Three-gluon Vertex

B. Allés^{a,1}, D.S. Henty^b, H. Panagopoulos^c, C. Parrinello^d, C. Pittori^e, D.G. Richards^{f,b}

^a Dipartimento di Fisica Università di Pisa
 Piazza Torricelli 2, 56126 Pisa, Italy

^b Dept. of Physics & Astronomy, University of Edinburgh,
 Edinburgh EH9 3JZ, United Kingdom
 (UKQCD Collaboration)

^c Department of Natural Sciences, University of Cyprus
 CY-1678 Nicosia, Cyprus

^d Dept. of Mathematical Sciences, University of Liverpool
 Liverpool L69 3BX, U.K.
 (UKQCD Collaboration)

^e L.P.T.H.E., Université de Paris Sud, Centre d'Orsay,
 91405 Orsay, France.

^f Fermilab, P.O. Box 500, Batavia, IL 60510, USA

Abstract

We compute the running QCD coupling on the lattice by evaluating two-point and three-point off-shell gluon Green's functions in a fixed gauge and imposing non-perturbative renormalisation conditions on them. Our exploratory study is performed in the quenched approximation at $\beta = 6.0$ on 16^4 and 24^4 lattices. We show that, for momenta in the range 1.8 – 2.3 GeV, our coupling runs according to the two-loop asymptotic formula, allowing a precise determination of the corresponding Λ parameter. The role of lattice artifacts and

¹Address after April 1997: Dipartimento di Fisica, Sezione Teorica, Università Degli Studi di Milano, Via Celoria 16, 20133-Milano, Italy.

finite-volume effects is carefully analysed and these appear to be under control in the momentum range of interest. Our renormalisation procedure corresponds to a momentum subtraction scheme in continuum field theory, and therefore lattice perturbation theory is not needed in order to match our results to the \overline{MS} scheme, thus eliminating a major source of uncertainty in the determination of $\alpha_{\overline{MS}}$. Our method can be applied directly to the unquenched case.

1 Introduction

The running coupling $\alpha_s(\mu)$, where μ is a momentum scale, is a fundamental QCD quantity providing the link between low and high-energy properties of the theory. Given a renormalisation scheme, $\alpha_s(\mu)$ can be measured experimentally for a wide range of momenta. A precise determination of $\alpha_s(\mu)$ (or equivalently of the scale Λ determining the rate at which α_s runs) is extremely important as it would fix the value of a fundamental parameter in the Standard Model, providing bounds on new physics.

Computing α_s is a major challenge for the lattice community. Several different lattice definitions of the renormalised coupling have so far been investigated [1, 2, 3, 4]. Apart from the static quark potential approach [3], which involves a phenomenological parametrisation of the interquark potential, one feature of all other definitions of the coupling is that lattice perturbation theory (LPTH) has been used in order to convert the measured numerical value into a value for $\alpha_{\overline{MS}}$. Despite recent proposals to improve the convergence of LPTH series [5], this step still provides one important source of systematic errors in the final prediction for $\alpha_{\overline{MS}}$. At present, systematic errors, namely quenching, discretisation effects, finite volume effects and LPTH, dominate statistical ones for state-of-the-art computations.

We investigate here a more recent proposal [6] for the determination of α_s from the renormalised three-gluon vertex. This is achieved by evaluating two-point and three-point off-shell Green's functions of the gluon field on the lattice, in the Landau gauge, and imposing non-perturbative renormalisation conditions on them, for different values of the external momenta. By varying the renormalisation scale μ , one can determine $\alpha_s(\mu)$ for different momenta from a single simulation and analyse the μ -dependence of the coupling. In particular, one can investigate if the asymptotic behaviour is reproduced for large momenta. In practice, for a given choice of the lattice parameters, one needs to choose μ in a range of lattice momenta such that both finite volume effects and discretisation errors are under control. If such a momentum region exists and if the coupling is found to run according to the two-loop asymptotic formula, then we can get a meaningful measurement of $\alpha_s(\mu)$ in our renormalisation scheme which can then be related perturbatively to other definitions of the coupling.

As will be explained in the following, a crucial feature of this procedure, which corresponds to momentum subtraction renormalisation in continuum QCD, is that renormalised Green's functions do not depend on the way the theory is regularised. As a consequence, LPTH is not needed in order to relate the measured coupling to $\alpha_{\overline{MS}}$, and the relation between the two schemes can be computed entirely in continuum perturbation theory. An analogous non-perturbative approach has been recently applied, with encouraging results, to the renormalisation of composite fermion operators [8].

The aim of this paper is to demonstrate the feasibility of our approach and to investigate the rôle of systematic lattice uncertainties, such as discretisation effects and volume dependence. We perform this investigation in the quenched approximation at $\beta = 6.0$ for two different lattice volumes. Given the simplicity of the method, we expect the application to full QCD to present no additional problems [7].

The paper is organised as follows: in Section 2 we present the renormalisation scheme, the definition of the coupling and the numerical procedure. In Section 3 we give the lattice results, discussing all sources of systematic errors in the calculation. In Section 4 we discuss the procedure to relate our coupling to $\alpha_{\overline{MS}}$ and we compare our non-perturbative results with predictions based on the use of LPTH. In Section 5 we summarise our work and we discuss some possible future developments. Finally, the details of the perturbative calculations are given in the appendix.

2 The Method

Provided systematic errors are under control, in order to compute $\alpha_{\overline{MS}}$ from the lattice it is sufficient to:

1. set the scale of momenta in physical units by determining the lattice spacing a ;
2. define a suitable renormalisation scheme and a renormalised coupling to be measured;
3. match the result to the \overline{MS} scheme.

The physical quantities most frequently used to determine the value of a are: the ρ meson mass, the string tension, the 1P-1S mass splitting in heavy quarkonia [1], and a characteristic length r_0 , phenomenologically connected to the intermediate range of the heavy quark potential [9]. Each choice has its theoretical and technical advantages, extensively discussed in the literature.

In this work we set $\beta = 6.0$ and we take the value of a^{-1} determined by Bali and Schilling [3] in their string tension measurements. These yield $a^{-1} = 1.9 \pm 0.1$ GeV. We quote a systematic error on the scale to take into account the uncertainty resulting from other possible choices.

The definition and measurement of the coupling is achieved by computing the gluon propagator and the three-gluon vertex function in a fixed gauge and renormalising them in a non-perturbative way. We define the lattice gluon field $A_\mu(x)$ as

$$A_\mu(x + \hat{\mu}/2) = \frac{U_\mu(x) - U_\mu^\dagger(x)}{2ia g_0} - \frac{1}{3} \text{Tr} \left(\frac{U_\mu(x) - U_\mu^\dagger(x)}{2ia g_0} \right), \quad (1)$$

where $\hat{\mu}$ indicates a unit lattice vector in the μ direction and g_0 is the bare coupling constant (we omit the colour index).

After performing the Fourier transform of (1) one can define (unrenormalised) lattice n -point gluon Green's functions, in momentum space:

$$G_U^{(n)}{}_{\mu_1 \mu_2 \dots \mu_n}(p_1, p_2, \dots, p_n) = \langle A_{\mu_1}(p_1) A_{\mu_2}(p_2) \dots A_{\mu_n}(p_n) \rangle, \quad (2)$$

where $\langle \cdot \rangle$ indicates the Monte-Carlo average and momentum conservation implies $p_1 + p_2 + \dots + p_n = 0$.

Since the lattice calculation aims to evaluate such Green's functions in the "continuum window", i.e. for a range of parameters such that continuum physics is observed, the following criteria must be satisfied:

1. $\beta \geq 6.0$, so that scaling is observed for physical quantities.
2. La is large enough in physical units, where L is the linear dimension of the lattice, such that finite-volume effects are under control.
3. Discretisation errors due to the contribution of nonleading terms in a^2 to the Green's functions are negligible.

Since we work in momentum space, the last requirement can be directly translated into a restriction on the range of lattice momenta that should be used. In the remainder of this section we assume that all the above requirements are met and we adopt the formalism of continuum QCD.

We choose to work in the Landau gauge. As already mentioned, the quantities of interest are the unrenormalised gluon propagator

$$G_U^{(2)}{}_{\mu\nu}(p) \equiv T_{\mu\nu}(p) G_U(p^2), \quad T_{\mu\nu}(p) \equiv \delta_{\mu\nu} - \frac{p_\mu p_\nu}{p^2} \quad (3)$$

and the complete unrenormalised gluon three-point function $G_U^{(3)}{}_{\alpha\beta\gamma}(p_1, p_2, p_3)$. This is related to the one-particle-irreducible three-point function $\Gamma_U^{(3)}{}_{\alpha\beta\gamma}(p_1, p_2, p_3)$ by the formula

$$G_U^{(3)}{}_{\alpha\beta\gamma}(p_1, p_2, p_3) \equiv \Gamma_U^{(3)}{}_{\delta\rho\xi}(p_1, p_2, p_3) G_U^{(2)}{}_{\delta\alpha}(p_1) G_U^{(2)}{}_{\rho\beta}(p_2) G_U^{(2)}{}_{\xi\gamma}(p_3). \quad (4)$$

In order to renormalise the gluon wave function, we impose that at a fixed momentum scale $p^2 = \mu^2$ the renormalised gluon propagator takes its continuum tree-level value. One gets the non-perturbative renormalisation condition

$$G_R(p)|_{p^2=\mu^2} = Z_A^{-1}(\mu a) G_U(pa)|_{p^2=\mu^2} = \frac{1}{\mu^2}. \quad (5)$$

The above equation defines in a non-perturbative way the gluon wave-function renormalisation Z_A .

For the three-gluon vertex, we start by choosing a kinematics suitable for the lattice geometry and which allows a simple non-perturbative definition of the vertex renormalisation constant Z_V . Recalling the general form of $\Gamma_U^{(3)}$ in the continuum [10], it turns out that if one evaluates $G_U^{(3)}$ in the Landau gauge at the kinematical points defined by

$$\alpha = \gamma, \quad p_1 = -p_3 = p, \quad p_2 = 0, \quad (6)$$

then one can write

$$\frac{\sum_{\alpha=1}^4 G_U^{(3)}{}_{\alpha\beta\alpha}(pa, 0, -pa)}{(G_U(pa))^2 G_U(0)} = 6 i Z_V^{-1}(pa) g_0 p_\beta. \quad (7)$$

With the above definition Z_V contains a term which is linear in the external momenta but not proportional to the tree-level vertex (see appendix). Notice

that the numerical calculation on the lattice for the three-gluon vertex yields directly the product $Z_V^{-1}g_0$.

At this point we can define the running coupling g at the scale μ from the renormalised three-gluon vertex at the asymmetric point as

$$g(\mu) = Z_A^{3/2}(\mu a) Z_V^{-1}(\mu a) g_0, \quad (8)$$

where the relevant renormalisation constants have been defined in (5), (7) and $\alpha_s(\mu) \equiv g(\mu)^2/4\pi$. This choice corresponds to a momentum subtraction scheme, usually referred to as \widetilde{MOM} in continuum QCD [11]. We postpone the discussion of the matching procedure until Section 4.

2.1 Computational Procedure

$SU(3)$ gauge configurations were generated at $\beta = 6.0$ at two lattice sizes; 150 configurations on a 16^4 lattice, and 103 configurations on a 24^4 lattice. The configurations on the smaller lattice were generated on a 16K CM-200 at the University of Edinburgh, using a hybrid-overrelaxed algorithm, where both Cabibbo-Marinari pseudo-heatbath and overrelaxed updates were performed on three $SU(2)$ subgroups. Successive configurations were separated by 150 sweeps (every sixth sweep a heat-bath), 1000 sweeps being allowed for thermalisation. Landau gauge-fixing was achieved by using a Fourier-accelerated algorithm [12]. Autocorrelations were investigated by performing a standard jackknife error analysis.

The data for the larger lattice were generated on the ACPMAPS supercomputer at FNAL using the Creutz pseudo-heatbath algorithm, with 1600 sweeps between configurations. The configurations were fixed to the Landau gauge using an overrelaxation algorithm, with the final iterations being performed in double precision.

A crucial step in the method is the accurate implementation of the lattice Landau gauge condition

$$\Delta(x) = \sum_{\mu} A_{\mu}(x + \hat{\mu}) - A_{\mu}(x) = 0. \quad (9)$$

To monitor the gauge-fixing accuracy we compute the quantity

$$\theta = \frac{1}{VN_C} \sum_x \text{Tr} \Delta^{\dagger}(x)\Delta(x) \quad (10)$$

as the algorithm progresses, terminating when $\theta < 10^{-11}$ (this is close to 32-bit machine precision). Since our calculations involve low momentum modes of gluon correlation functions, the above test is not in itself sufficient because $\Delta(x)$ is a local quantity. For this reason, we also compute

$$A_0(t) = \sum_{\vec{x}} A_0(\vec{x}, t). \quad (11)$$

In a periodic box, the Landau gauge condition implies that $A_0(t)$ is independent of t [13]. In particular, for our configurations on the smaller lattice, $A_0(t)$ was constant to better than one part in 10^5 . For the purpose of our analysis, the only quantity that needs to be stored is the Fourier-transformed field $A_\mu(p)$ for a selected range of lattice momenta. All n -point gluon correlation functions can then be assembled using eq. (2), where momentum conservation is imposed explicitly.

To compute α_s , we first evaluate the gluon propagator and determine Z_A from eq. (5). Next, we measure the complete three-point function $G_U^{(3)}$ of the gluon field and the quantity on the l.h.s. of (7). Finally, $g(\mu)$ is obtained from eq. (8). We take advantage of all the symmetries of the problem to improve statistics. The quoted errors are obtained using a single-point-elimination jackknife algorithm.

3 Results

3.1 Tensor Structure

We start by analysing the tensor structure of the lattice gluon propagator and three-gluon vertex function as a means both of determining the degree of violation of continuum rotational invariance, and of verifying the extent to which the Landau gauge condition is satisfied in momentum space.

It is worth noting that our definition (1) for the gluon field differs from the one which has been used in all non-perturbative calculations to date, which is [13]:

$$A'_\mu(x) = \frac{U_\mu(x) - U_\mu^\dagger(x)}{2iag_0} - \frac{1}{3} \text{Tr} \left(\frac{U_\mu(x) - U_\mu^\dagger(x)}{2iag_0} \right). \quad (12)$$

It turns out that the above “asymmetric” definition is not consistent with the one which is usually used in perturbative lattice calculations. Consistency is achieved by using the “symmetric” definition (1), which has better properties in the continuum limit. To illustrate this point, we observe that in momentum space the two definitions are related by the formula

$$A_\mu(p) = e^{-ip_\mu/2} A'_\mu(p). \quad (13)$$

If we now write the Landau gauge-fixing condition (9) in momentum space, using the asymmetric definition one gets

$$\sum_\mu [(\cos p_\mu - 1) - i \sin p_\mu] A'_\mu(p) = 0, \quad (14)$$

while the symmetric definition yields

$$\sum_\mu 2i \sin p_\mu/2 A_\mu(p) = 0. \quad (15)$$

In the limit $a \rightarrow 0$ the continuum gauge condition is recovered with $O(a)$ corrections in the asymmetric case and $O(a^2)$ in the symmetric one. Thus the latter corresponds to an “improved” lattice Landau gauge condition.

By using the symmetric definition one can check very accurately the tensor structure of non-perturbative lattice Green’s functions against what is expected from LPTH. Based on such a definition we expect the Landau gauge propagator to satisfy

$$G_U^{(2)}{}_{\mu\nu}(p) = \hat{T}_{\mu\nu}(\hat{p}) G_U(\hat{p}^2), \quad \hat{T}_{\mu\nu}(\hat{p}) \equiv \delta_{\mu\nu} - \frac{\hat{p}_\mu \hat{p}_\nu}{\hat{p}^2}, \quad (16)$$

where

$$\hat{p}_\mu = \frac{2}{a} \sin\left(\frac{p_\mu a}{2}\right). \quad (17)$$

This makes the analysis of violations of rotational invariance very simple since, if our propagator is found to satisfy (16), one has for any $p \neq 0$:

$$\sum_\mu G_U^{(2)}{}_{\mu\mu}(p) = 3 G_U(\hat{p}^2), \quad (18)$$

so that violations of rotational invariance in $\sum_\mu G_U^{(2)}{}_{\mu\mu}(p)$ can only arise from the scalar part $G_U(p^2)$. If the asymmetric definition is used, the simple

p	$\frac{p_0}{p_1}$	$\frac{\sin p_0/2}{\sin p_1/2}$	$-\frac{G_{01}}{G_{00}}$	$\frac{p_1}{p_0}$	$\frac{\sin p_1/2}{\sin p_0/2}$	$-\frac{G_{01}}{G_{11}}$	$\frac{p_1^2}{p_0^2}$	$\frac{\sin^2 p_1/2}{\sin^2 p_0/2}$	$\frac{G_{00}}{G_{11}}$
(1, 1, 0, 0)	1	1	1.00	1	1.0	1.00	1	1.0	1.00
(1, 2, 0, 0)	1/2	0.510	0.510	2	1.962	1.962	4	3.849	3.848
(2, 2, 0, 0)	1	1	1.00	1	1.0	1.00	1	1.0	1.00
(1, 3, 0, 0)	1/3	0.351	0.351	3	2.848	2.848	9	8.110	8.110
(3, 3, 0, 0)	1	1	1.00	1	1.0	1.00	1	1.0	1.00

Table 1: Symmetry tests for $G_U^{(2)}{}_{\mu\nu}(p)$ on the 16^4 lattices at $\beta = 6.0$, using the symmetric definition of A_μ .

p	$\frac{p_0}{p_1}$	$\frac{\sin p_0/2}{\sin p_1/2}$	$-\frac{G_{01}}{G_{00}}$	$\frac{p_1}{p_0}$	$\frac{\sin p_1/2}{\sin p_0/2}$	$-\frac{G_{01}}{G_{11}}$	$\frac{p_1^2}{p_0^2}$	$\frac{\sin^2 p_1/2}{\sin^2 p_0/2}$	$\frac{G_{00}}{G_{11}}$
(1, 1, 0, 0)	1	1	1.00	1	1	1.00	1	1	1.00
(1, 2, 0, 0)	1/2	0.510	0.50	2	1.962	1.924	4	3.848	3.848
(2, 2, 0, 0)	1	1	1.00	1	1	1.00	1	1	1.00
(1, 3, 0, 0)	1/3	0.351	0.324	3	2.848	2.631	9	8.110	8.110
(3, 3, 0, 0)	1	1	1.00	1	1	1.00	1	1	1.00

Table 2: Symmetry tests for $G_U^{(2)}{}_{\mu\nu}(p)$ on the 16^4 lattices at $\beta = 6.0$, using the asymmetric definition of A_μ .

tensor structure in eq. (16) is modified and the interpretation of the numerical results is more difficult.

In Tables 1 and 2 we show ratios of tensor components of the gluon propagator on the 16^4 lattices using the symmetric and asymmetric definitions of A_μ respectively. These are compared to what is expected from (16) and its continuum counterpart. In all cases the uncertainty is less than one unit in the last quoted figure. We note the following:

- For the symmetric definition of A_μ , the numerical data are completely consistent with our expectation from eq. (16). This indicates that the lattice gauge condition has been implemented very accurately, so that we have a complete understanding of the tensor structure of the two-

point function.

- For the asymmetric definition of A_μ , the picture is quite different, although even in this case the deviation from (16) is at most 10% for the momenta shown.

We consider now the three-gluon correlator $G_U^{(3)}{}_{\alpha\beta\gamma}(p, 0, -p)$. On the lattice we expect it to satisfy

$$G_U^{(3)}{}_{\alpha\beta\gamma}(p, 0, -p) = \hat{T}_{\alpha\gamma}(\hat{p}) F(\hat{p}^2) \hat{p}_\beta (G_U(\hat{p}^2))^2 G_U(0), \quad (19)$$

which is the form one obtains by performing the substitution $p_\mu \rightarrow \hat{p}_\mu$ in the continuum expression. Here $F(\hat{p}^2)$ represents a generic function of \hat{p}^2 . Note that from (13) it follows that $G_U^{(3)}{}_{\alpha\beta\gamma}(p, 0, -p)$ does not depend on the definition used for the gauge field as the extra phase factor associated with the symmetric definition of $A_\mu(p)$ cancels at this kinematic point.

In Tables 3 and 4 we show ratios of tensor components of $G_U^{(3)}{}_{\alpha\beta\gamma}(p, 0, -p)$ on the 16^4 and 24^4 lattices compared to expectations from (19) and its continuum counterpart.

p	$\frac{p_1^2}{p_0^2}$	$\frac{\sin^2 p_1/2}{\sin^2 p_0/2}$	$\frac{G_{010}}{G_{111}}$	$\frac{p_0}{p_1}$	$\frac{\sin p_0/2}{\sin p_1/2}$	$\frac{G_{101}}{G_{111}}$	$\frac{p_1}{p_0}$	$\frac{\sin p_1/2}{\sin p_0/2}$	$-\frac{G_{011}}{G_{111}}$
(1, 1, 0, 0)	1	1	1.000	1	1	1.1(2)	1	1	1.000
(1, 2, 0, 0)	4	3.848	3.848	1/2	0.510	0.3(1)	2	1.962	1.962
(2, 2, 0, 0)	1	1	1.000	1	1	0.8(3)	1	1	1.000

Table 3: Symmetry tests for $G_U^{(3)}{}_{\alpha\beta\gamma}(p, 0, -p)$ in the Landau gauge, using the symmetric definition of A_μ , on 16^4 lattices. Unless otherwise noted, the error is always less than one unit in the last quoted figure.

The theoretical expectation is satisfied very accurately for two of the three ratios under consideration, while the agreement for the ratio G_{101}/G_{111} is much poorer, especially on the larger lattice. This is related to the fact that the first two ratios are completely determined by the Landau gauge condition for our choice of the momenta, whilst the last ratio is not. Thus these

p	$\frac{p_2^2}{p_0^2}$	$\frac{\sin^2 p_1/2}{\sin^2 p_0/2}$	$\frac{G_{010}}{G_{111}}$	$\frac{p_0}{p_1}$	$\frac{\sin p_0/2}{\sin p_1/2}$	$\frac{G_{101}}{G_{111}}$	$\frac{p_1}{p_0}$	$\frac{\sin p_1/2}{\sin p_0/2}$	$-\frac{G_{011}}{G_{111}}$
(1, 1, 0, 0)	1	1	1.000	1	1	-0.3(4)	1	1	1.000
(1, 2, 0, 0)	4	3.932	3.932	1/2	0.504	-0.2(4)	2	1.983	1.983
(2, 2, 0, 0)	1	1	1.000	1	1	0.3(7)	1	1	1.000
(1, 3, 0, 0)	9	8.596	8.596	1/3	0.341	0.8(7)	3	2.932	2.932

Table 4: Symmetry tests for $G_U^{(3)}{}_{\alpha\beta\gamma}(p, 0, -p)$ in the Landau gauge, using the symmetric definition of A_μ , on 24^4 lattices. Unless otherwise noted, the error is always less than one unit in the last quoted figure.

results provide further evidence that the momentum-space Landau gauge-fixing condition is very well satisfied on all our lattices, but they also hint at a poorer quality of the data on the larger lattice.

3.2 Renormalisation Constants and Running Coupling

We are now left with the task of computing the renormalisation constants defined in (5) and (7) and the running coupling (8). Notice that because of our definitions and choice of kinematics, the difference between the symmetric and asymmetric definitions for the gauge field is immaterial for this purpose. All data are plotted vs. $\mu = \sqrt{p^2}$, expressed in GeV. In order to detect violations of rotational invariance, we have used whenever possible different combinations of lattice vectors for a fixed value of p^2 and we have plotted separately the corresponding data points.

In Figure 1 we show the scalar gluon self-energy $G_U(\mu)$. Statistical errors are negligible and no violations of rotational invariance can be detected in the momentum range under consideration. Next we compute the gluon three-point function and evaluate the running coupling according to (8). This is plotted in Figure 2 for both lattice sizes. We obtain again a clear signal; on the other hand, the data do show some violations of rotational invariance. We note again that the errors on the 24^4 lattice are considerably larger than on the smaller lattice.

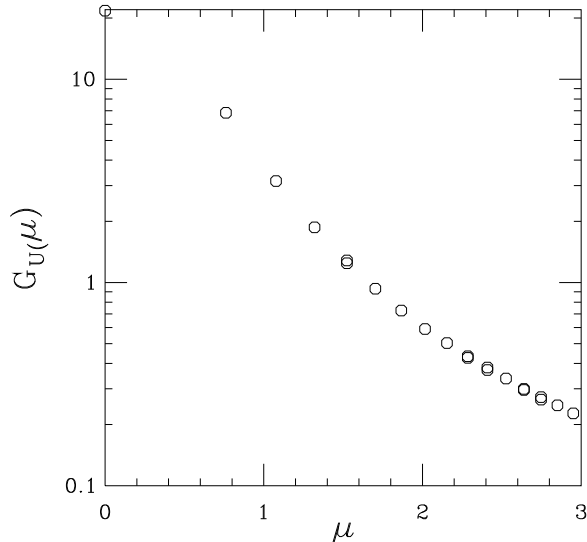


Figure 1: $G_U(\mu)$ vs. μ for the 16^4 lattices at $\beta = 6.0$.

3.3 Systematic Lattice Uncertainties and Extraction of Λ

The important physical question is whether one can isolate a range of momenta where lattice artifacts are negligible and our coupling runs according to the two-loop perturbative expression

$$g^2(\mu) = \left[b_0 \ln(\mu^2/\Lambda_{\widetilde{MOM}}^2) + \frac{b_1}{b_0} \ln \ln(\mu^2/\Lambda_{\widetilde{MOM}}^2) \right]^{-1}, \quad (20)$$

where $b_0 = 11/16\pi^2$, $b_1 = 102/(16\pi^2)^2$ and $\Lambda_{\widetilde{MOM}}$ is the QCD scale parameter for the renormalisation scheme that we are using (in the quenched approximation). To answer this question, and obtain an estimate for $\Lambda_{\widetilde{MOM}}$, we compute $\Lambda_{\widetilde{MOM}}$ as a function of the measured values of $g^2(\mu)$ according to the formula

$$\Lambda_{\widetilde{MOM}} = \mu \exp\left(-\frac{1}{2b_0g^2(\mu)}\right) \left[b_0g^2(\mu)\right]^{-\frac{b_1}{2b_0^2}}. \quad (21)$$

If the coupling runs according to (20), then $\Lambda_{\widetilde{MOM}}$ as defined from the above equation must be constant. Given the exponential dependence of $\Lambda_{\widetilde{MOM}}$ on $g^2(\mu)$, this test is a very stringent one. As an alternative procedure one could fit the data for $g^2(\mu)$ to formula (20), with $\Lambda_{\widetilde{MOM}}$ as a parameter, but this

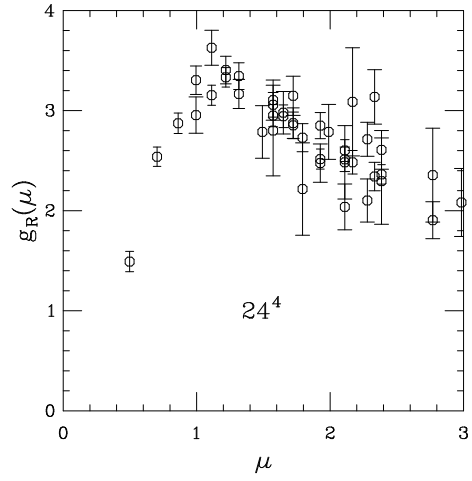
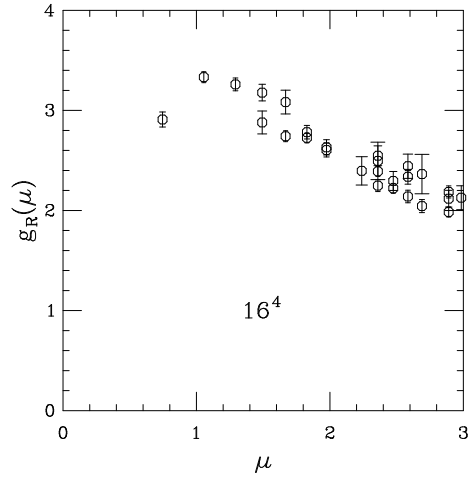


Figure 2: Running coupling $g(\mu)$ vs. μ .

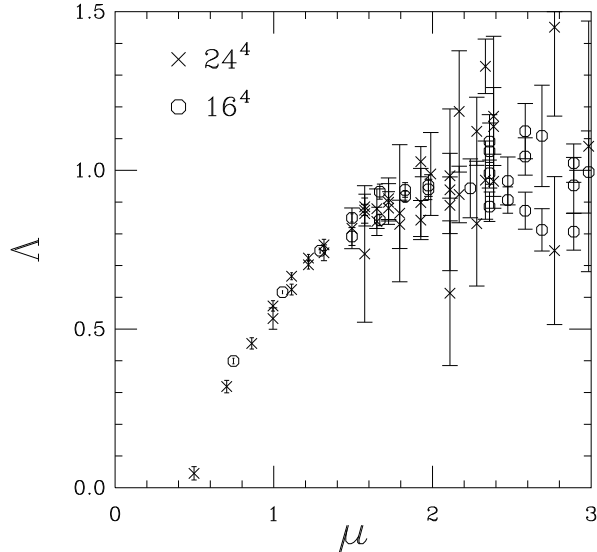


Figure 3: $\Lambda_{\widetilde{MOM}}$ vs. μ for our two lattice sizes.

would not result in a strong test since (20) only depends logarithmically on $\Lambda_{\widetilde{MOM}}$.

By plotting $\Lambda_{\widetilde{MOM}}$ versus μ (see Figure 3), three different regimes can be identified:

1. For $\mu < 1.8$ GeV, $\Lambda_{\widetilde{MOM}}$ displays a strong dependence on the renormalisation scale. This is not surprising, as for low momenta asymptotic scaling is not expected.
2. In the range $1.8 < \mu < 2.3$ GeV the data are consistent with a constant value for $\Lambda_{\widetilde{MOM}}$. No violations of rotational invariance are observed in such a range and a comparison of the two lattice sizes shows no volume dependence either. This is shown in Figure 4.
3. For $\mu > 2.3$ GeV, rotational invariance is broken by higher order terms in a^2 and the two-loop behaviour disappears.

In summary, we appear to have a “continuum window” in the range $1.8 < \mu < 2.3$ GeV, where two-loop scaling is observed and lattice artifacts are under control. In order to extract a prediction for $\Lambda_{\widetilde{MOM}}$, we fit the data points in the continuum window to a constant. We take as our best estimate

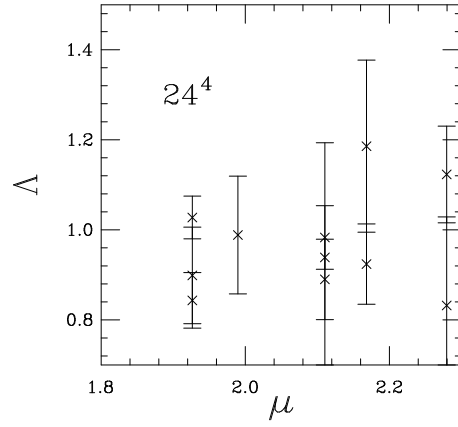
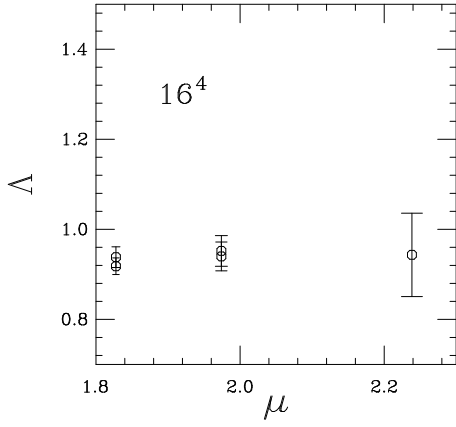


Figure 4: $\Lambda_{\widetilde{MOM}}$ vs. μ in the “continuum window”.

the fit to the 16^4 data, for which the statistical errors are smaller, and obtain

$$\Lambda_{\widetilde{MOM}} = 0.96 \pm 0.02 \pm 0.09 \text{ GeV}, \quad (22)$$

where the first error is statistical and the second error comes from the uncertainty on the value of a^{-1} .

Since our lattice calculation is performed in a fixed gauge, it is worth mentioning that non-perturbative gauge-fixing ambiguities (Gribov copies) may in principle affect our results. These could be regarded as a potential source of systematic errors. However, based on previous investigations of other lattice gauge-fixed quantities[14], we believe that the contribution of ‘‘Gribov noise’’ to the overall error, if at all present, is negligible.

4 Matching to \overline{MS}

In this section we extract a prediction for $\alpha_{\overline{MS}}$ with zero active quark flavours from our numerical results for $\Lambda_{\widetilde{MOM}}$. As already mentioned, the procedure that we adopt avoids the use of LPTH. We also discuss a LPTH calculation which provides some important consistency checks.

We start from our numerical estimate (22) of the continuum scale parameter $\Lambda_{\widetilde{MOM}}$. The general relation between the scale parameters in two continuum schemes A and B can be written as

$$\frac{\Lambda_A}{\Lambda_B} = \exp\left[-\frac{1}{2b_0}\left(\frac{1}{g_A^2(\mu)} - \frac{1}{g_B^2(\mu)}\right) + O(g^2(\mu))\right], \quad (23)$$

with

$$g_A^2(\mu) = g_B^2(\mu)\left(1 + \frac{g_B^2(\mu)}{4\pi}C_{AB} + O(g_B^2(\mu))\right), \quad (24)$$

where C_{AB} , which in general depends on the chosen gauge and on the number of active flavours, is obtained from a continuum perturbative calculation as described in the appendix. Since Λ_A , Λ_B are independent of μ and because of asymptotic freedom, by letting $\mu \rightarrow \infty$ the ratio (23) can be determined to all orders in the coupling constant from the one-loop calculation (see for example [15, 16]).

We obtain, in the Landau gauge and for zero quark flavours

$$\frac{\Lambda_{\overline{MS}}^{(0)}}{\Lambda_{\widetilde{MOM}}^{(0)}} = 0.35. \quad (25)$$

This result is in agreement with previous one-loop calculations of the three-gluon vertex [17].

Note that the scheme that we have adopted for the non-perturbative calculation (see Section 2) differs from the usual \widetilde{MOM} scheme as it contains an extra constant term in the vertex renormalisation constant. This is a linear term in the momenta, not proportional to the tree level vertex, which is equal on the lattice and in the continuum. The coefficient in (25) includes it perturbatively (see appendix).

Using (22) and (25), we can extract $\Lambda_{\overline{MS}}^{(0)}$ from

$$\Lambda_{\overline{MS}}^{(0)} = \Lambda_{\widetilde{MOM}}^{(0)} \frac{\Lambda_{\overline{MS}}^{(0)}}{\Lambda_{\widetilde{MOM}}^{(0)}}. \quad (26)$$

We get

$$\Lambda_{\overline{MS}}^{(0)} = 0.34 \pm 0.05 \text{ GeV}. \quad (27)$$

This is the main result of our computation.

Our result can be directly compared with the one of ref. [3]:

$$\Lambda_{\overline{MS}}^{(0)} = 0.293 \pm 0.018_{-0.063}^{+0.025} \text{ GeV}. \quad (28)$$

In terms of $\alpha_{\overline{MS}}^{(0)}$, our result yields:

$$\alpha_{\overline{MS}}^{(0)}(2.0 \text{ GeV}) = 0.25 \pm 0.02. \quad (29)$$

We do not attempt to estimate $\alpha_{\overline{MS}}^{(n_f)}$ for $n_f \neq 0$ on the basis of quenched data; a computation in full QCD with two degenerate flavours of sea quarks is in progress.

4.1 Starting from the Lattice

One can apply renormalisation group considerations, analogous to the ones that establish the momentum dependence of the renormalised coupling, to the bare theory. On the lattice, as in any other regularisation scheme, renormalisability implies that the bare coupling constant should be cut-off dependent and, for a small enough, $g_0 = g_0(a)$ should be a universal function of a . Thus in the scaling region one can define, up to an arbitrary integration constant, an a -independent Λ_{LATT} parameter, in terms of the lattice spacing and of the bare lattice coupling as

$$\Lambda_{LATT} = \frac{1}{a} \exp\left(\int^{g_0(a)} \frac{dg'_0}{\beta(g'_0)}\right). \quad (30)$$

In the asymptotic scaling region $a \rightarrow 0$ and $g_0(a) \rightarrow 0$, where the β -function is perturbatively computable, one can fix the integration constant by defining Λ_{LATT} as

$$\Lambda_{LATT} = \frac{1}{a} \exp\left(-\frac{1}{2b_0 g_0^2(a)}\right) (b_0 g_0^2(a))^{-\frac{b_1}{2b_0^2}}, \quad (31)$$

independent of a in the asymptotic scaling limit. Note that, whereas we find asymptotic scaling for the renormalised coupling for momenta $1.8 < q < 2.3$ GeV, see eq. (21) and Figure 3, this does not necessarily imply that the asymptotic regime has already set in for the bare coupling used in the simulation. As a check, which involves lattice perturbation theory, we can

1. take the non-perturbative determination of $\Lambda_{\widetilde{MOM}}$,
2. compute the ratio $\Lambda_{LATT}/\Lambda_{\widetilde{MOM}}$ in lattice perturbation theory
3. extract Λ_{LATT} from

$$\Lambda_{LATT} = \Lambda_{\widetilde{MOM}} \frac{\Lambda_{LATT}}{\Lambda_{\widetilde{MOM}}} \quad (32)$$

and compare the value obtained from eq. (32) with the one from eq. (31).

The ratio

$$\frac{\Lambda_{\widetilde{MOM}}}{\Lambda_{LATT}} = \mu a \exp\left[-\frac{1}{2b_0} \left(\frac{1}{g_{\widetilde{MOM}}^2(\mu)} - \frac{1}{g_0^2(a)}\right) + O(g_0^2)\right] \quad (33)$$

has been calculated at one-loop by Hasenfratz and Hasenfratz [11] in the Feynman gauge $\lambda = 1$, where λ here is the gauge parameter. They found

$$\frac{\Lambda_{\widetilde{MOM}}(\lambda = 1)}{\Lambda_{LATT}} = 69.4. \quad (34)$$

We have checked their result by working in a general covariant gauge. The details of the LPTH calculation are given in the appendix. In the Landau gauge, we get

$$\frac{\Lambda_{\widetilde{MOM}}(\lambda = 0)}{\Lambda_{LATT}} = 54.6. \quad (35)$$

The number that we need to insert in (32) is not quite the above one, because of the already mentioned extra term in the vertex renormalisation, not proportional to the tree level vertex. In our scheme the result is

$$\frac{\Lambda_{\widetilde{MOM}}(\lambda = 0)}{\Lambda_{LATT}} = 83.2. \quad (36)$$

By inserting it into eq. (32), and using the result (22), one would get

$$\Lambda_{LATT} = 11.6 \text{ MeV}, \quad (37)$$

to be compared with

$$\Lambda_{LATT} = 4.5 \text{ MeV} \quad (38)$$

obtained from the hypothesis of asymptotic scaling, eq. (31), with $g_0^2 = 1$ and $a^{-1} = 1.9 \text{ GeV}$. The comparison confirms the well known result that for values of β accessible to current simulations, Λ_{LATT} still displays β dependence [3]. We stress again that in our case the matching procedure, described in the previous subsection, does not require knowledge of Λ_{LATT} .

Another way of seeing the failure of LPTH in this case is to compare the non-perturbative results for $g^2(\mu)$ with what is obtained by inserting in the relation

$$g^2(\mu) = Z_A^3(\mu a) Z_V^{-2}(\mu a) g_0^2(a) \quad (39)$$

the values of the Z 's obtained in LPTH and “boosted” lattice perturbation theory [5]. This comparison is shown in Figure 5.

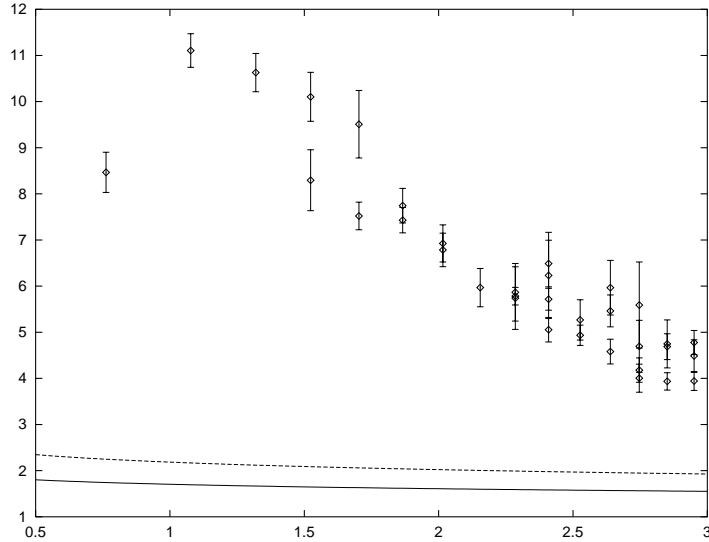


Figure 5: $g^2(\mu)$ vs. momentum as evaluated non-perturbatively on the 16^4 lattice and from standard (solid line) and boosted (dashed line) LPTH.

Finally, we can perform a cross-check of our perturbative calculations on the lattice and in the continuum as follows. It is known [18] that at the one-loop level

$$\frac{\Lambda_{\overline{MS}}}{\Lambda_{LATT}} = 28.8. \quad (40)$$

This is a gauge-invariant quantity, since $\Lambda_{\overline{MS}}$ and Λ_{LATT} are both gauge independent. We can insert in the identity

$$\left(\frac{\Lambda_{\overline{MS}}}{\Lambda_{\widetilde{MOM}(\lambda)}}\right)\left(\frac{\Lambda_{\widetilde{MOM}(\lambda)}}{\Lambda_{LATT}}\right) = \frac{\Lambda_{\overline{MS}}}{\Lambda_{LATT}} \quad (41)$$

our continuum result for $\Lambda_{\overline{MS}}/\Lambda_{\widetilde{MOM}}$ and the lattice one for $\Lambda_{\widetilde{MOM}}/\Lambda_{LATT}$, which we have evaluated for a generic covariant gauge. For any value of λ we get indeed the value (40) found in the literature.

5 Conclusions

We have shown in the pure gauge theory that a non-perturbative determination of the QCD running coupling can be obtained from first principles by a

lattice study of the triple-gluon vertex. We have some evidence that systematic lattice effects are under control in our calculation. The main features of our method are that LPTH is not needed to match our results to \overline{MS} and that the extension to the full theory does not present in principle any extra problem. Encouraged by our results in the quenched approximation, we are now repeating our calculation with dynamical quarks.

6 Acknowledgements

The numerical work was carried out on the Connection Machine 200 at the University of Edinburgh, and on the Fermilab lattice supercomputer, ACPMAPS. B. Allés acknowledges an Italian INFN postdoctoral fellowship. D. Henty, C. Parrinello and D. Richards acknowledge the support of PPARC through a Personal Fellowship (DH), Advanced Fellowships (CP and DGR), and grant GR/J 21347 (CP). C. Pittori acknowledges the support of an HCM Individual Fellowship ER-BCHBICT930887. This work was supported in part by the DOE under contract DE-AC02-76CH03000.

We thank C. Michael, O. Pène and G.C. Rossi for many helpful suggestions and for reading the manuscript. We also thank J.I. Skullerud for some help with the numerical work.

7 Appendix

We start by giving the details of the (quenched) one-loop continuum perturbative calculation needed to relate the scale parameter Λ in the \overline{MOM} scheme to the one in \overline{MS} .

The three-gluon vertex in the \overline{MS} scheme, calculated at the asymmetric point and at $p^2 = \mu^2$, can be written in a generic covariant gauge as (we suppress colour indices)

$$\begin{aligned} \Gamma_{\overline{MS} \alpha\beta\gamma}^{(3)}(p/\mu, 0, -p/\mu)|_{p^2=\mu^2} &= \left[1 + \frac{g^2}{16\pi^2} C_V(\lambda) \right] \Gamma_{tree \alpha\beta\gamma}^{(3)}(p, 0, -p) \\ &+ i \frac{g^3}{16\pi^2} C_{extra}(\lambda) \left[\delta_{\alpha\gamma} p_\beta - \frac{p_\alpha p_\beta p_\gamma}{p^2} \right], \end{aligned} \quad (42)$$

where λ is the gauge parameter and

$$\begin{aligned} C_V(\lambda) &= \frac{3}{2} \left[\frac{61}{18} + \frac{1}{2} \lambda^2 \right], \\ C_{extra}(\lambda) &= \frac{3}{2} \left[-\frac{37}{6} + 3\lambda + \frac{1}{2} \lambda^2 \right]. \end{aligned} \quad (43)$$

The (Euclidean) tree-level vertex is

$$\Gamma_{tree \alpha\beta\gamma}^{(3)}(p, 0, -p) = -ig \left[\delta_{\alpha\beta} p_\gamma + \delta_{\gamma\beta} p_\alpha - 2\delta_{\alpha\gamma} p_\beta \right]. \quad (44)$$

Note that despite the vanishing of one of the external momenta, the renormalised vertex (42) is a finite quantity, as the infrared behaviour is completely controlled by the off-shell gluon [17].

Setting $\alpha = \gamma$ and summing over α we get

$$\begin{aligned} \sum_{\alpha} \Gamma_{\overline{MS} \alpha\beta\alpha}^{(3)}(p/\mu, 0, -p/\mu)|_{p^2=\mu^2} &= \\ 6igp_\beta \left[1 + \frac{g^2}{16\pi^2} \left(C_V(\lambda) + \frac{C_{extra}(\lambda)}{2} \right) \right]. \end{aligned} \quad (45)$$

Whereas in the \overline{MS} scheme only the pole part appears in the definition of renormalisation constants, nontrivial finite terms are included in momentum

subtraction schemes. In particular, in our \widetilde{MOM} scheme the finite combination $(C_V + C_{extra}/2)$, which appears in eq. (45), enters in the definition (7) of Z_V . Hence, by computing

$$g^2(\mu) = Z_A^3(\epsilon, \mu) Z_V^{-2}(\epsilon, \mu) g_0^2(\epsilon) \quad (46)$$

in the two schemes, one finds that the coefficient $C_{\overline{MS}, \widetilde{MOM}}$, which relates the two couplings according to (24), is given by the expression

$$C_{\overline{MS}, \widetilde{MOM}} = -\frac{1}{4\pi} \left[3C_A(\lambda) - 2 \left(C_V(\lambda) + \frac{C_{extra}(\lambda)}{2} \right) \right], \quad (47)$$

where

$$C_A(\lambda) = 3 \left[\frac{97}{36} + \frac{1}{2}\lambda + \frac{1}{4}\lambda^2 \right] \quad (48)$$

is the finite contribution coming from the gluon self-energy at one-loop [15]. By setting $\lambda = 0$, we obtain the result in the Landau gauge

$$C_{\overline{MS}, \widetilde{MOM}} = -1.856807669\dots \quad (49)$$

Finally, the ratio (25) of the Λ parameters is obtained from

$$\frac{\Lambda_{\overline{MS}}^{(0)}}{\Lambda_{\widetilde{MOM}}^{(0)}} = \exp \left[\frac{C_{\overline{MS}, \widetilde{MOM}}}{8\pi b_0} \right] = 0.35, \quad (50)$$

where $b_0 = \frac{11}{16\pi^2}$ in the quenched approximation.

Turning now to our lattice calculations, we observe that the part of the one-loop three-gluon vertex on the lattice that is proportional to the tree-level vertex can be written as

$$\begin{aligned} \Gamma_L^{(3)} &= \Gamma_{\text{tree}}^{(3)} \times \left(1 + g_0^2 A_L \right) \\ &= \Gamma_{\text{tree}}^{(3)} \times \left(1 + g_0^2 A_{\overline{MS}} + g_0^2 C_L \right), \end{aligned} \quad (51)$$

where A_L and $A_{\overline{MS}}$ stand for the (momentum dependent) lattice and continuum (\overline{MS} scheme) contributions respectively. The quantity C_L , which relates the pure lattice result to the \overline{MS} scheme, is momentum independent. Extra terms not proportional to the tree-level vertex are equal on the lattice and in the continuum, thus they do not contribute to C_L , which can be computed by evaluating the diagrams of Figure 6.

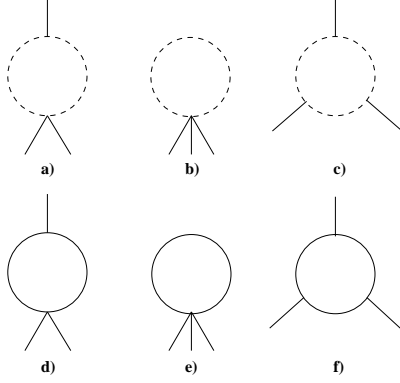


Figure 6: Diagrams for the one-loop three-gluon vertex on the lattice. Dashed and solid lines indicate ghosts and gluons respectively.

The contribution of each one to C_L is

$$\begin{aligned}
\text{a)} &= 0 \\
\text{b)} &= 0 \\
\text{c)} &= \frac{N}{24} \left(\frac{1}{16\pi^2} L - \frac{1}{4} J + \frac{1}{6} Z_0 \right) \\
\text{d)} &= \frac{N}{4} \left(\frac{9}{16\pi^2} L - \frac{9}{4} J - \frac{3}{16} + \frac{143}{48} Z_0 \right) + \\
&\quad (1 - \lambda) \frac{N}{8} \left(-\frac{3}{16\pi^2} L + \frac{3}{4} J - \frac{13}{8} Z_0 \right) \\
\text{e)} &= \frac{1}{8N} - N \left(\frac{1}{64} + \frac{5}{8} Z_0 \right) + (1 - \lambda) N \frac{11}{96} Z_0 \\
\text{f)} &= \frac{N}{8} \left(-\frac{13}{16\pi^2} L + \frac{13}{4} J - \frac{13}{8} Z_0 + \frac{16}{96\pi^2} \right) + \\
&\quad (1 - \lambda) \frac{N}{8} \left(\frac{9}{16\pi^2} L - \frac{9}{4} J + \frac{23}{24} Z_0 \right). \tag{52}
\end{aligned}$$

In these equations L , Z_0 and J are [19, 20]

$$L \equiv \ln \mu^2 a^2 + \gamma_{\text{euler}} - \ln 4\pi$$

$$\begin{aligned}
Z_0 &\equiv \int_{-\pi}^{+\pi} \frac{d^4q}{(2\pi)^4} \frac{1}{\hat{q}^2} = 0.1549333902311, \\
J &\equiv 0.0465621749414.
\end{aligned}
\tag{53}$$

Finally μ is the mass scale introduced during the dimensional regularisation of the continuum \overline{MS} scheme. These formulae are valid for the gauge group $SU(N)$. Notice that both A_L and $A_{\overline{MS}}$ depend on λ , λ^2 and λ^3 , while C_L depends only on λ .

Collecting all contributions in eq. (52), we obtain the result for C_L

$$\begin{aligned}
C_L &= \frac{1}{8N} + \frac{2}{3}N \left(\frac{1}{16\pi^2}L - \frac{1}{4}J - \frac{11}{96}Z_0 - \frac{3}{32} + \frac{1}{32\pi^2} \right) + \\
&\quad (1-\lambda)\frac{3}{4}N \left(\frac{1}{16\pi^2}L - \frac{1}{4}J + \frac{1}{24}Z_0 \right).
\end{aligned}
\tag{54}$$

Now, using the results of reference [17] we get the result for A_L in the Landau gauge

$$A_L = \frac{17}{4} \frac{1}{16\pi^2} \ln p^2 a^2 - 0.294728.
\tag{55}$$

References

- [1] A.X. El-Khadra et al., Phys. Rev. Lett. 69 (1992) 729.
- [2] M. Lüscher et al., Nucl. Phys. B413 (1994) 481.
- [3] G.S. Bali and K. Schilling, Phys. Rev. D47 (1993) 661.
- [4] S.P. Booth et al., Phys. Lett. B294 (1992) 385.
- [5] G.P. Lepage, P.B. Mackenzie, Phys. Rev. D48 (1993) 2250.
- [6] C. Parrinello, Phys. Rev. D50 (1994) 4247.
- [7] UKQCD Collaboration (in progress).
- [8] G. Martinelli, C. Pittori, C.T. Sachrajda, M. Testa, A. Vladikas, Nucl. Phys. B445 (1995) 81.

- [9] R. Sommer, Nucl. Phys. B411 (1994) 839.
- [10] J.S. Ball, T.W. Chiu, Phys. Rev. D22 (1980) 2550.
- [11] A. Hasenfratz, P. Hasenfratz, Phys. Lett. B93 (1980) 165.
- [12] C.T.H. Davies et al., Phys. Rev. D37 (1988) 1581.
- [13] J.E. Mandula, M. Ogilvie, Phys. Lett. B185 (1987) 127.
- [14] The concept of “Gribov noise” was introduced in: M.L. Paciello et al., Phys. Lett. B289 (1992) 405. For studies in the Landau gauge see, for example, M.L. Paciello et al., Phys. Lett. B341 (1994) 187 and A. Cucchieri, hep-lat/9705005.
- [15] W. Celmaster and R.J. Gonsalves, Phys. Rev. D20 (1979) 1420.
- [16] A. Billoire, Phys. Lett. B104 (1981) 472.
- [17] F.T. Brandt and J. Frenkel, Phys. Rev. D33 (1986) 464.
- [18] R. Dashen and D.J. Gross, Phys. Rev. D23 (1981) 2340
- [19] H. Kawai, R. Nakayama and K. Seo, Nucl. Phys. B 189 (1981) 40.
- [20] A. González-Arroyo and C.P. Korthals Altes, Nucl. Phys. B 205 (1982) 46.